

# Perspective: Strongly correlated and topological states in [111] grown transition metal oxide thin films and heterostructures

Jak Chakhalian,<sup>1, a)</sup> Xiaoran Liu,<sup>1, b)</sup> and Gregory A. Fiete<sup>2, 3, c)</sup>

<sup>1)</sup>*Department of Physics, Rutgers University, Piscataway, New Jersey 08854-8019, USA*

<sup>2)</sup>*Department of Physics, Northeastern University, Boston, Massachusetts 02115, USA*

<sup>3)</sup>*Department of Physics, Massachusetts Institute of Technology, Cambridge, Massachusetts 02139, USA*

(Dated: 30 March 2020)

We highlight recent advances in the theory, materials fabrication, and experimental characterization of strongly correlated and topological states in [111] oriented transition metal oxide thin films and heterostructures, which are notoriously difficult to realize compared to their [001] oriented counterparts. We focus on two classes of complex oxides, with the chemical formula  $ABO_3$  and  $A_2B_2O_7$ , where the B sites are occupied by an open-shell transition metal ion with a local moment, and the A sites are typically a rare earth. The [111] oriented quasi-two-dimensional lattices derived from these parent compound lattices can exhibit peculiar geometries and symmetries, namely, a buckled honeycomb lattice, as well as kagome and triangular lattices. These lattice motifs form the basis for emergent strongly correlated and topological states expressed in exotic magnetism, various forms of orbital ordering, topological insulators, topological semimetals, quantum anomalous Hall insulators, and quantum spin liquids. For transition metal ions with high atomic number, spin-orbit coupling plays a significant role and may give rise to additional topological features in the electronic band structure and in the spectrum of magnetic excitations. We conclude the Perspective by articulating open challenges and opportunities in this actively developing field.

## I. INTRODUCTION

Physicists undertake a continuous quest for high quality quantum materials in the thin-film form that harbor interesting many-body phases and are tunable by substrate strain, dimensional control, and compositional modulation. Such systems typically allow for the realization of a complex many-body ground state with multiple entwined correlated and topological states that may—in principle—be tuned as a function of external control parameters, such as external electric and magnetic fields, optical excitations, gating, and pressure.

Over the past decade, transition metal oxide interfaces have been a subject of intense investigation with the prime focus on the complex oxides in the  $ABO_3$  perovskite form (here A is typically a rare earth element, B is an open-shell transition metal element, and O is oxygen). These thin films and heterostructures are predominantly grown along the [001] direction<sup>1–8</sup>. As a vivid illustration of the physical possibilities, some of the [001] oriented interfaces composed of two insulating materials show the emergence of a two-dimensional electron gas (2DEG) with electronic states derived primarily from the  $d$ -orbitals of the transition metal ions<sup>9–11</sup>, rather than the more extended and less weakly correlated  $s$ ,  $p$ -orbitals common to semiconductor interfaces. Compared to the extremely high mobility of carriers in GaAs/AlGaAs heterostructures used to study the fractional quantum Hall effect<sup>12</sup>, the 2DEGs at the [001] oxide interfaces have significantly lower mobility but exhibit markedly stronger electron-electron correlations<sup>13–19</sup> that enable a richer set of compelling phenomena including the

quantum Hall effect<sup>20</sup>, the fractional quantum Hall effect<sup>21</sup>, unconventional superconductivity<sup>22–24</sup>, and magnetism<sup>24,25</sup>. The large variety of accessible states in these systems can potentially usher in a new era of oxide electronics that exploit these correlated states<sup>26,27</sup>.

In this Perspective, we focus on a new direction which is still in its infancy – transition metal oxide films templated in high-index (e.g. [111]) directions. Compared to the [001] direction, growth along [111] is more difficult due to the lack of readily available lattice-matched substrates, and less favorable and generally little understood thermodynamics of such growth. The first step in this direction was taken with the  $ABO_3$  perovskites, both on the theoretical<sup>28–32</sup> and experimental sides<sup>33–35</sup>. An important motivator was the theoretical prediction that correlated topological states, such as the quantum anomalous Hall state, could be realized in ultra-thin films of [111] oriented perovskites<sup>36</sup>, where the transition metal ions in a bilayer system form a buckled honeycomb lattice. This was an important step because the honeycomb lattice has played a pivotal role in the pioneering theoretical studies of topological states on lattices<sup>37–39</sup>.

While the perovskite systems are interesting in their own right, in this Perspective we also focus on the interesting class of compounds  $A_2B_2O_7$  which brings an additional element of geometrical frustration, compared to the  $ABO_3$  materials. In  $A_2B_2O_7$  compounds, the B sites form a pyrochlore lattice—a network of corner sharing tetrahedra. Viewed along the [111] direction, the lattice consists of alternating kagome and triangular lattice planes. Both the kagome and triangular lattices lead to magnetic frustration, which can support exotic fractionalized states—a major motivation for experimentally achieving high quality materials growth for such systems. The three-dimensional pyrochlore lattice is fully frustrated as well, and can give rise to fractionalized topological insulators<sup>40</sup> and topologically ordered magnetic states such as quantum spin

<sup>a)</sup>Electronic mail: jak.chakhalian@rutgers.edu.

<sup>b)</sup>Electronic mail: xiaoran.liu@rutgers.edu.

<sup>c)</sup>Electronic mail: g.fiete@northeastern.edu.

liquids<sup>41</sup>, which may portend what is possible with the thin-film versions highlighted in this Perspective.

This Perspective is organized as follows. In Sec.II we describe several theoretical proposals for novel electronic states and experimental results in the [111] grown ABO<sub>3</sub> perovskite bilayer, which exhibits a buckled honeycomb lattice. In Sec.III we describe theoretical proposals for novel electronic states and experimental results on [111] oriented A<sub>2</sub>B<sub>2</sub>O<sub>7</sub>. We highlight the challenges of the A<sub>2</sub>B<sub>2</sub>O<sub>7</sub> pyrochlore growth compared to the heavily investigated films of the ABO<sub>3</sub> family. Finally, in Sec.IV, we conclude with an outlook towards possible future routes to investigation of these quantum materials.

We note that we do not aim to present a comprehensive review of this fast moving field, but rather provide our perspective of the challenges and opportunities in this direction. We apologize to those whose work is not prominently featured here or inadvertently omitted.

## II. [111] GROWN ABO<sub>3</sub> BILAYER: A BUCKLED HONEYCOMB LATTICE

Conventionally, perovskite films and heterostructures are synthesized along the pseudo-cubic [001] direction. As seen in Fig.1, films grown along the [001] direction consist of alternating AO and BO<sub>2</sub> atomic planes. The same perovskite viewed along the [111] direction exhibits alternating AO<sub>3</sub> and B planes. Interestingly, by growing *two* pseudo-cubic unit cells of ABO<sub>3</sub> along [111], one can generate an entirely new type of lattice with two vertically shifted triangular planes of B sites (see Fig. 1(b)). This artificially assembled buckled honeycomb lattice provides a unique opportunity to explore new phenomena due to the superposition of complex *d*-orbitals in a graphene-like setting.

What is the reason for such a dramatic change in the many-body ground state caused by the new lattice motif? To start, we note that both tight-binding models and first-principles calculations indicate that *d*-electrons constitute the majority of states at the Fermi level<sup>28–31,42–44</sup>. Here we focus on the partially filled shells with *e<sub>g</sub>* electrons. Unlike [001] oriented perovskites that strongly favor real orbitals, in [111] *d*-orbitals possess *d*-wave symmetry (e.g.  $|d \pm id\rangle = (|d_{z^2}\rangle \pm i|d_{x^2-y^2}\rangle)/\sqrt{2}$ ) in the orbital space, which in a sufficiently weakly interacting regime also favor complex orbital orderings<sup>31</sup>. In addition, for quarter-filling (e.g. low-spin  $3d^7$ ), the Fermi level lies right at the  $\Gamma$ -point where two bands touch quadratically forming a so called “quadratic band crossing” (QBC) point<sup>28,29,31</sup>. Moreover, *six-fold symmetry* at the QBC point protects it against splitting into Dirac points<sup>45</sup>. Finally, since in the *e<sub>g</sub>* manifold orbital angular momentum is quenched, the spin-orbit interaction only enters via mixing with *t<sub>2g</sub>*-orbitals in the higher-order terms<sup>46</sup>. These features (the orbital structure of the states, along with the electronic band structure) set the stage for non-trivial theoretical possibilities.

Specifically, due to the buckled graphene-like periodic arrangement of atoms, theoretical calculations for [111]-oriented bilayers of nickelates have predicted the realization of several exotic phases unattainable in either bulk or [001]-oriented

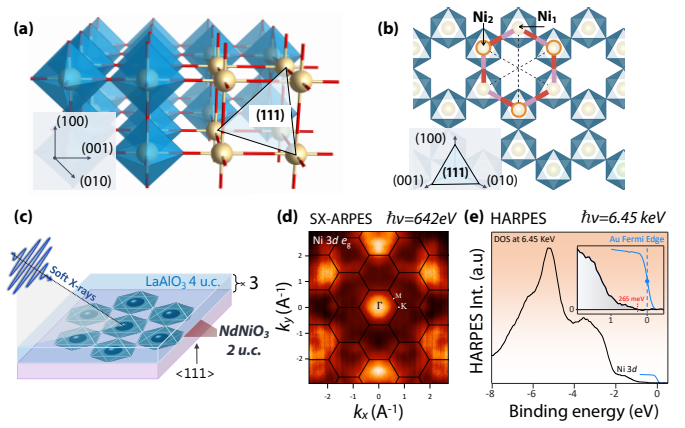


FIG. 1. (a) Two unit cells of an infinite layer perovskite lattice ABO<sub>3</sub> viewed along the <100> direction. A-site and oxygen atoms are omitted for clarity. (b) The same structure when grown along <111> forms a graphene-like lattice with two sub-lattices and a buckled O-B-O bond. (c) Schematic diagram of the soft x-ray angle resolved photoemission spectroscopy (SX-ARPES) and hard x-ray photoemission spectroscopy (HARPES) experimental geometry and the sample structure. (d) Momentum resolved SX-ARPES photoemission intensity map for LaNiO<sub>3</sub> of the Ni 3d states near the valence-band maximum measured with the photon energy of 642 eV. (e) Bulk-sensitive HARPES spectrum recorded at a photon energy of 6.45 keV with the estimated probing depth of approximately 85 Å. Inset shows a high-statistics spectrum of the valence-band maximum (at the binding energy of 265 meV), referenced to the Au Fermi edge (Figures (c)-(e) adapted from Ref.[47]).

heterojunctions<sup>28–31,42–44,48</sup>. For instance, model Hamiltonian calculations in the strongly correlated limit predicted that orbital ordering wins spontaneously over the bulk-like charge-ordered phase, whereas in the weakly correlated limit, a number of topological phases, including the Dirac half-metal phase, the quantum anomalous Hall insulator phase, and spin nematic phase with weak ferromagnetism, all *driven by interactions without explicitly large spin-orbit coupling*, are feasible.<sup>28,29,31</sup> The details of these theoretical possibilities have appeared earlier in Ref.[36].

Despite numerous predictions of interesting electronic and topological phases, the number of experimentally realized [111] lattice structures is very limited<sup>49</sup>. To understand this situation, first we remind the reader that the majority of popular perovskite substrates (e.g. SrTiO<sub>3</sub>, LaAlO<sub>3</sub>, NdGaO<sub>3</sub>, and YAlO<sub>3</sub>) are polar along [111] with alternating +4e/-4e (or +3e/-3e) charges per unit cell for each atomic plane. The large surface charges present a challenge, particularly because the process of initial nucleation and epitaxy on such high energy surfaces is not well understood. In addition, [111] grown bi-layers of perovskites readily demonstrate complex combinations of structural, chemical, and electronic reconstructions, which necessarily develop to compensate for the large electric fields from the polarity jump<sup>49–51</sup>. It is important to emphasize that unlike bulk crystals or thicker films, these imperfections in morphology and electronic structure are naturally amplified in a graphene-like monolayer of the material. The presence of

top and bottom interfaces which are epitaxially coupled to the active monolayer constitutes another often poorly-understood control parameter.

To shed light on those issues, monolayer-by-monolayer growth has been investigated by monitoring *in-situ* reflection high-energy electron diffraction (RHEED) during the growth progression of  $\text{LaNiO}_3$  on  $\text{SrTiO}_3$  (a polar interface) and  $\text{LaNiO}_3$  on  $\text{LaAlO}_3$  (a non-polar interface) for the case of [111]-oriented substrates<sup>52</sup>. The results revealed that in the polar case a non-perovskite  $\text{La}_2\text{Ni}_2\text{O}_5$  phase rapidly develops within the first five unit cells followed by a gradual recovery of the desired  $\text{LaNiO}_3$  phase. In sharp contrast, high-quality stoichiometric [111]  $\text{LaNiO}_3$  was successfully stabilized on the  $\text{LaAlO}_3$  [111] surface; these findings imply that a key to successful [111] growth is in a judicious choice of a film/substrate combination to avoid the polar mismatch at the interface<sup>35</sup>.

In close connection, we can conjecture that a few unit cells of a metallic or semiconducting buffer grown next to the ionic polar surface (e.g.  $\text{SrRuO}_3$ ,  $\text{SrVO}_3$ ) may rapidly screen those charges and internal electric fields to enable layer-by-layer synthesis even in the highly polar cases. This attractive approach, however, may cause ambiguity in the detection and interpretation of emerging metallic states in thin film against a trivial contribution from the conducting buffer layer.

The experimental determination of the electronic, magnetic and structural properties of monolayer thick materials is another demanding venue. Following theoretical predictions<sup>28-31,42-44</sup>, the behavior of  $3d^7$  electrons on the buckled honeycomb lattice was investigated by resonant soft x-ray absorption on a high quality [111] bilayer of  $\text{NdNiO}_3$  capped by 4 unit cells  $\text{LaAlO}_3$  templated on a  $\text{LaAlO}_3$  [111] substrate. A detailed analysis of the angular dependent linear dichroism revealed the presence of a new ground state characterized by antiferromagnetic correlations and orbital ordering, unattainable in either bulk  $\text{NdNiO}_3$  or in analogous heterostructures layered along the conventional (001) direction<sup>53</sup>.

Furthermore, electronic band structure characterization by Angle Resolved PhotoEmission Spectroscopy (ARPES) of an active buried monolayer presents an immense technical challenge and yet is highly desired because it is the most direct probe of topological band structures. The main obstacle standing in the way of such measurements is the fact that conventional probes of electronic structure including ARPES or scanning tunneling spectro-microscopy (STM) are severely limited in their applicability to such systems due to the high surface-sensitivity.

Motivated by these challenges, novel bulk- and buried-layer-sensitive spectroscopic and scattering techniques, such as soft x-ray angle resolved photoemission spectroscopy (SX-ARPES)<sup>54,55</sup> and hard x-ray photoemission spectroscopy (HAXPES)<sup>56,57</sup>, have recently emerged as viable probes for comprehensive investigations of ultrathin buried layers and interfaces due to their enhanced probing depth<sup>58</sup>.

For instance, recently, Arab *et al.* applied a combination of SX-ARPES and HAXPES to obtain the momentum-resolved and angle-integrated valence-band electronic structure of an ultrathin buckled graphene-like layer of [111]  $\text{NdNiO}_3$  confined between two 4-unit cell-thick layers of insulating  $\text{LaAlO}_3$

(see Fig.1c)<sup>47</sup>. The direct measurements of the momentum-resolved electronic dispersion of the near-Fermi-level Ni  $3d$  valence states via SX-ARPES (shown in Fig.1d) provided an unambiguous evidence of such antiferro-orbital order and revealed a  $P1$  structural symmetry arrangement in a  $1 \times 1$  unit cell, consistent with the results suggested by the x-ray linear dichroism (XLD) data<sup>53</sup>. Complementary angle-integrated HAXPES measurements of the bulk-sensitive valence-band density of states (shown in Fig.1e) revealed the presence of a small bandgap of 265 meV, consistent with theoretical predictions. These early results suggest an effective strategy for investigating engineered states of matter even in buried structures of only a few atomic layers thick.

The rather thorough experimental investigation of [111] grown bilayers of  $\text{NdNiO}_3$  did not provide evidence for a non-trivial topological state, the most likely of which would be a QAHE state<sup>29,30</sup>. The null experimental result for the topological phase detection is somewhat surprising given that even the inclusion of realistic lattice distortions, such as the rotations of octahedral cages of oxygens surrounding the Ni ions, were included in the calculations and showed no important effect on the presence of topological states<sup>30</sup>.

Our best assessment of why the QAHE state was not realized is that the phase requires a rather fine balance of the on-site interaction energy and Hund's exchange coupling on the Ni atoms<sup>29,30</sup>. The precise values of these quantities are difficult to determine since they depend in detail on the way the system is modeled. In particular, theoretical models typically use a "down folding" scheme in which higher-energy bands are "integrated out" but taken into account in the low-energy models with effective on-site interaction and Hund's coupling<sup>59</sup>. The higher bands result in a screening effect that reduces the effective interaction and exchange values (which are the ones appearing in a few band model) compared to their "bare" values in a model that includes all the bands from all the atoms. The predicted topological phase lies in a rather narrow range of the on-site interaction and Hund's coupling, and the material may happen to fall out of this range. Another possibility is that the relatively small band gap predicted by theory is overwhelmed by disorder effects in the bilayer systems and magnetic domains form instead of a pristine topological state.

### III. [111] PYROCHLORE LATTICE

While the  $\text{ABO}_3$  perovskite systems are interesting in their own right, the  $\text{A}_2\text{B}_2\text{O}_7$  pyrochlore systems bring in an addition element in the form of geometrical frustration. In these materials, the B sites form a pyrochlore lattice - a network of corner sharing tetrahedra. As seen in Fig.2(d), when viewed along the [111] direction the lattice consists of alternating kagome and triangular lattice planes. Both the kagome and triangular lattices give rise to the phenomenon of magnetic frustration, which can result in exotic fractionalized states with quantum numbers of the electron (such as spin and charge) broken apart or broken down into smaller values<sup>40,41,60</sup>.

The bulk crystal pyrochlore systems have gathered significant attention from both the magnetism<sup>61-64</sup> and the correlated

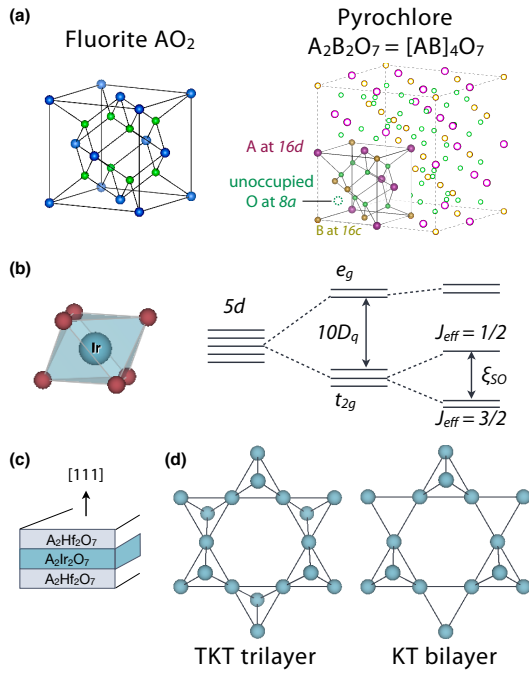


FIG. 2. (a) Lattice of the pyrochlore materials considered in this Perspective, exhibiting close resemblance to the fluorite structure. (b) Crystal field environment for  $A_2Ir_2O_7$ . (b) The Ir atom sits inside an octahedral cage of oxygen ions  $O^{2-}$  which results in a splitting  $10D_q$  of the  $d$ -levels into an upper  $e_g$  manifold and a lower  $t_{2g}$  manifold. Spin-orbit coupling  $\xi_{SO}$  further splits the  $t_{2g}$  levels into  $J_{\text{eff}} = 3/2$  and  $J_{\text{eff}} = 1/2$  states. For many pyrochlore compounds, the  $J_{\text{eff}} = 1/2$  states are half-filled. If the spin-orbit coupling is large enough, one may retain only these states in a low-energy model for a qualitative description. (c) A sandwich structure of a  $[111]$  oriented film showing a thin layer capped by two insulators  $A_2Hf_2O_7$  with a large band gap. (d) The alternating triangular-kagome-triangular (TKT), trilayer (T) and kagome-triangular (KT) bilayer lattice structure viewed along the  $[111]$  direction. These geometrically frustrated lattices can host multiple emergent correlated and topological electronic states.

topological insulator communities<sup>40,65–75</sup>. Of particular interest to this Perspective are the pyrochlore iridates,  $A_2Ir_2O_7$ . In this compound the Ir atom has an outer  $d$ -shell with 5 electrons, and sits in an approximately cubic environment, leading to a splitting of the  $5d$  orbital into a subset of lower-lying  $t_{2g}$  orbitals and higher lying  $e_g$  orbitals, as depicted in Fig.2(b). For heavy elements, like Ir, the spin-orbit coupling is sufficiently strong to lock the spin and angular momentum together producing an effective total angular momentum  $J_{\text{eff}} = 3/2$  and  $J_{\text{eff}} = 1/2$ , though there may be some degree of mixing when the spin-orbit coupling is large<sup>46</sup>. Five electrons in the  $d$ -shell thus corresponds to a half-filled  $J_{\text{eff}} = 1/2$  state, and parallels can be made to spin 1/2 systems. This feature entwined with the frustrated lattice is a major motivator for theoretical studies of the pyrochlore iridates and osmates.

An important general consideration for topological states is the spatial dimension of the system. Certain topological states, such as Weyl semimetals exist in three spatial dimensions, but not two<sup>76</sup>. Thus, the film thickness is an important parameter

in the realization of topological states. In the ultra-thin limit, the system is effectively two-dimensional and states such as the QAHE (a zero magnetic field quantum Hall state) are possible. For spin systems (local moments on the lattice), the spatial dimension is also important—the lower the dimension, the larger the quantum fluctuations and hence the easier to achieve even more exotic magnetic ground states such as quantum spin liquids<sup>41,77</sup>.

It is important to note that the vast amount of literature over the last 15 years on topological band structures is largely a subset of what are now referred to more generally as “symmetry protected topological” states or SPT states. For example, time-reversal invariant topological insulators with a non-trivial  $Z_2$  invariant require the imposition of time-reversal symmetry to provide a sharp distinction from trivial band insulators with a trivial  $Z_2$  invariant<sup>78–80</sup>. Topological crystalline insulators require some additional lattice symmetries, such as a mirror symmetry in the lattice that gives rise to a mirror Chern number, to provide a sharp distinction between the topological and non-topological phases<sup>81,82</sup>. There have also been studies of non-symmorphic space groups<sup>83,84</sup>, and many other discrete symmetries<sup>85,86</sup>.

The three-dimensional Weyl and Dirac systems, which have garnered much interest lately also require certain symmetries to be present for their realization and/or stability. Specifically, the Dirac metals require a four-dimensional irreducible representation of the small groups at specific momenta (for symmetry protection)<sup>87,88</sup>, and the Weyl systems entail either inversion symmetry or time-reversal symmetry breaking<sup>76</sup>. Another important way a Dirac metal can occur is at the phase boundary between a time-reversal invariant topological insulator and a trivial insulator<sup>89,90</sup>. These topological semimetals and their other variants, such as nodal line semimetals, have been reviewed recently<sup>76,91</sup>.

On the experimental front, the ability to grow such pyrochlore systems in thin-film form along the  $[111]$  direction offers opportunities to “design” interacting topological materials. In particular, *en route* to the two-dimensional limit from the three-dimensional limit, one may encounter “hidden” topological states<sup>92</sup> in the electronic band structure. There is now a rather vast literature on predicted topological states in  $[111]$  grown pyrochlore iridate thin films<sup>92–97</sup>, and other related systems<sup>28–31,36,42–44,98–107</sup>. As we mentioned in the introduction, it is not our intent to provide a comprehensive review, but rather highlight the richness of possibilities in this system.

The fabrication of  $A_2Ir_2O_7$  thin films and heterostructures remains extremely challenging due to the existence of several closely related critical issues. To understand them, it is necessary to emphasize the structural and chemical peculiarities of the pyrochlore iridates. First, pyrochlore oxides host geometrically frustrated interpenetrating A and B sublattices, such that the pyrochlore structure can be regarded as an anion-deficient fluorite structure ( $A_2B_2O_7 = [AB]_4O_7$ ), whose A and B cations alternatively occupy the fluorite cation sites along the  $\langle 110 \rangle$  direction, as illustrated in Fig. 2a. The anion vacancies reside in the tetrahedral interstices between adjacent B-site cations. As a result, defects can naturally enter into the structure, forming

off-stoichiometric phases  $A_{2\pm x}B_{2\pm y}O_{7\pm\delta}$ . Unfortunately, the electronic properties of pyrochlore iridates are very sensitive to the non-stoichiometry; For example, in  $\text{Eu}_2\text{Ir}_2\text{O}_7$ , approximately  $\sim 4\%$  of extra Ir is sufficient to entirely suppress the metal-insulator transition<sup>108</sup>.

Another formidable issue lies in the oxidation of iridium, which forms highly volatile gaseous iridium oxides (e.g.  $\text{IrO}_3$ ) during the growth. This elicits a dramatic loss of Ir inside the film<sup>109,110</sup>. The inherent Ir volatility acts to strongly magnify the formation of defects, further deviating the structure from the pyrochlore phase towards multiple secondary chemical phases. Here we emphasize that these issues are inherent to growth with all platinum metals, including gaseous phases of platinum, rhodium, iridium, ruthenium and osmium oxides<sup>111</sup>.

Therefore, to stabilize high quality films, one may naturally attempt to grow the films in high vacuum and at low temperature. However, this in turn triggers two other problems. First, due to the low reactivity of Ir metal,  $\text{Ir}^{4+}$  oxidation can only be achieved with great difficulty in the vacuum environment. Secondly, growing materials at low temperatures yields samples with very poor morphological quality.

With the growth challenges described above, layer-by-layer growth of [111]-oriented pyrochlore iridate ultra-thin films has yet to be demonstrated. Nevertheless, significant advances in the fabrication of [111]  $A_2\text{Ir}_2\text{O}_7$  thin films ( $A = \text{Nd}^{112,113}$ ,  $\text{Eu}^{114,115}$ ,  $\text{Tb}^{116,117}$ ,  $\text{Pr}^{118-120}$ ,  $\text{Bi}^{121-123}$ ) and heterostructures<sup>124</sup> have been steadily demonstrated.

The vast majority of the successfully grown  $A_2\text{Ir}_2\text{O}_7$  thin films have been realized via the so-called ‘‘solid phase epitaxy’’. In this method an amorphous film of the proper stoichiometry is first deposited on a [111]-oriented yttria-stabilized zirconia (YSZ) substrate by pulsed laser deposition or sputtering at reduced temperature and under low-oxygen partial pressure of pure  $\text{O}_2$  or  $\text{Ar}/\text{O}_2$  mixture, followed by *ex-situ* post-annealing at elevated temperatures to crystallize the amorphous film into the desired pyrochlore structure. Such a two-step growth protocol allows for the fabrication of reasonably high-quality  $A_2\text{Ir}_2\text{O}_7$  films down to a few tens of nanometers albeit with mediocre surface roughness. It should be noted that the growth window for each specific compound is rather narrow, lacks universality, and requires dedicated optimization<sup>112,114,121</sup>.

It is noteworthy that the films obtained by the ‘‘solid phase epitaxy’’ technique exhibit distinctly different transport behaviors from their bulk counterparts. In the bulk most of the  $A_2\text{Ir}_2\text{O}_7$  compounds show a metal-insulator transition (MIT) (except for  $A = \text{Pr}$  and  $\text{Bi}$ , which are pure metals)<sup>125</sup>. Concurrent with the MIT, the paramagnetic phase transits into an antiferromagnetic phase with the peculiar all-in-all-out (AIAO) spin configuration stabilized on each cation sublattice. Such a spin configuration has two degenerate domain structures – all-in-all-out (AIAO) and all-out-all-in (AOAI) – that are ‘switchable’ by time-reversal operation<sup>126</sup>.

Strikingly, not found in bulk, an unusual odd-parity field-dependent term in the magnetoresistance, together with a zero-field offset in the Hall resistance were lately discovered in [111]  $\text{Eu}_2\text{Ir}_2\text{O}_7$  thin films below the onset of the MIT<sup>114</sup>. Since the  $\text{Eu}^{3+}$  ion is non-magnetic, the observed exotic phenomena directly reflect the magneto-transport response of the carriers

coupled to the localized moments of the Ir sublattice. Specifically, it was argued to originate from the formation of the single AIAO domain defined by the direction of the cooling magnetic field. The observed magnetic domains are exceptionally rigid and once established, switching of domains can no longer be realized by sweeping experimentally accessible external fields<sup>115</sup>.

On the other hand, in pyrochlore iridates with *magnetic*  $A^{3+}$  ions, because of the strong magnetic coupling between  $4f$  and  $5d$  moments, switching of the Ir domains is easily accomplished by sweeping the external magnetic field along the [111] direction<sup>127</sup>. The proposed mechanism of domain switching has been captured in [111]  $\text{Tb}_2\text{Ir}_2\text{O}_7$  thin films<sup>116,117</sup>. Interestingly, the effect of domain switching leads to the formation of domain walls in the  $\{111\}$  planes, where two-fold rotational symmetry can be broken. As the result, an intrinsic anomalous Hall conductance due to non-zero Berry curvature may be probed at the domain walls. This phenomenon was recently demonstrated in [111]  $\text{Nd}_2\text{Ir}_2\text{O}_7$  thin films<sup>113</sup>, as well as at the [111] heterointerface between two pyrochlore iridates,  $\text{Eu}_2\text{Ir}_2\text{O}_7$  and  $\text{Tb}_2\text{Ir}_2\text{O}_7$ <sup>124</sup>.

In addition, for all metallic  $A_2\text{Ir}_2\text{O}_7$ , a spontaneous Hall effect (i.e. anomalous Hall effect without net magnetization) due to the spin chirality associated with  $\text{Pr}$   $4f$  moments was previously reported in bulk  $\text{Pr}_2\text{Ir}_2\text{O}_7$  below 1.5 K<sup>128</sup>. Surprisingly, the onset of the spontaneous Hall effect has been recently reported to appear at 50 K<sup>118</sup> or 15 K<sup>119</sup> in [111]  $\text{Pr}_2\text{Ir}_2\text{O}_7$  thin films – a temperature much higher than the spin-correlation scale due to  $\text{Pr}$  moments. Based on these results, the enhancement was speculated to originate from the Ir  $5d$  moments. One argument given by Ohtsuki *et al.* suggests that [111] epitaxial strain may induce the AIAO magnetic order on the Ir sublattice causing a magnetic Weyl semimetal state to appear in the film<sup>118</sup>. However, as no magnetic reflections associated with the AIAO order were detected by resonant scattering, Guo *et al.* argued that the spontaneous magnetization is likely due to the localization of the Ir moments, which either creates additional spin chirality or strengthens the effective  $\text{Pr}$ - $\text{Pr}$  coupling via the  $4f$  -  $5d$  interaction<sup>119</sup>. Additionally, linear magneto-resistance (MR) linked to the multiple types of charge carriers was found in [111]  $\text{Bi}_2\text{Ir}_2\text{O}_7$  thin films, exhibiting striking resemblances to the scale invariant MR in the strange metal state of high  $T_c$  cuprates<sup>121-123</sup>.

At this point, the conclusion we draw from these findings in  $A_2\text{Ir}_2\text{O}_7$  films is that the magnetic properties are significantly more complex than those of the corresponding bulk systems. The relative abundance of transport data can be contrasted to the challenges of performing other kinds of advanced measurements. For instance, magnetic neutron scattering is difficult because of the small number of scatterers to get a strong scattering signal and the fact that Ir is a strong neutron absorber<sup>129</sup>. The application of ARPES and STM is challenging due to the problem of *in-situ* preparing clean and atomically smooth surfaces of pyrochlore films. Furthermore, the potentially rich physics of *collective excitations* in thin films of Ir pyrochlores is almost entirely unexplored. This is primarily due to the low sample volume (e.g. for inelastic neutrons) and lack of momentum information for probes with high energy resolution



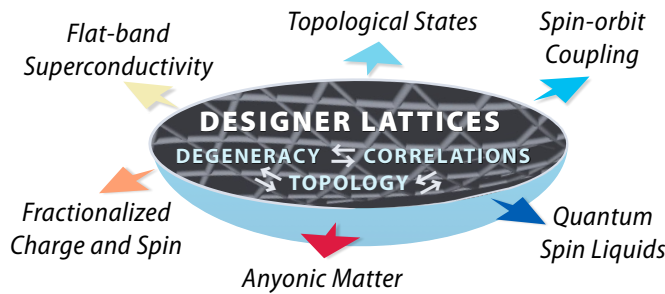


FIG. 3. Possible new quantum states and many-body phenomena that emerge on designer lattices, where the element of geometrical frustration is introduced.

(e.g. optical probes). One method that may prove to be sufficiently powerful for these systems is the resonant inelastic x-ray scattering (RIXS) which shows a strong response for Ir<sup>130</sup>.

#### IV. OUTLOOK

In this short Perspective, we have highlighted some of the key theoretical ideas motivating the drive to produce high quality [111] transition metal oxide thin films. One major point is that the material conditions are ripe for exotic many-body quantum states with topological properties or fractionalized excitations. On the experimental side, we have attempted to lay out some of the key materials fabrication challenges facing thin film growth. We hope our discussion will help other researchers to grasp gaps in our current understanding and see them as attractive opportunities to explore.

We will conclude the Perspective by looking into a possible future. From the materials side, while the current focus is mainly on perovskite and pyrochlore [111] oxides with active *d* electrons, systems dominated by *f* electrons can potentially lead to striking electronic and magnetic properties, especially where the *d-f* interaction is strong. In addition, this methodology can also be applied to structures with more interactive degrees of freedom<sup>131</sup>.

One of the promising candidates is the family of spinels AB<sub>2</sub>X<sub>4</sub>, in which both the A and B sites can be either magnetic or non-magnetic, and the X sites may be an element from the chalcogen family (group 16 of the periodic table). In this structure [111] quasi-two-dimensional slab is composed of alternating stacking of kagome and triangular cation planes with magnetic frustration, leading to the potentially rich and exotic magnetism<sup>132</sup>. Following the same line of thought, we can envision that the current scarcity of high quality Kitaev magnets can be mitigated by the designer approach akin to the graphene lattice derived from [111] perovskites. Finally, a large class of frustrated compounds with tri-fold symmetry including jarosites, wurtzites, and garnets await to be stabilized in the thin film form and investigated for interesting quantum and topological phases<sup>133</sup>.

All in all, as sketched in Fig. 3, designer lattices such as the

kagome and other thin film systems with geometrical frustration discussed in this Perspective, offer a new framework to explore some of the most interesting frontiers in contemporary condensed matter physics. Among those, the captivating possibilities of interacting topological states, quantum spin liquids, anyonic matter, fractionalized charge and spin fermions, and flat band superconductivity still lie in wait for their realization.

#### ACKNOWLEDGMENTS

The authors deeply acknowledge D. Khomskii, P. Coleman, P. Chandra, M. Kareev, J. Freeland and J. Pixley for insightful discussions. JC and XL were supported by the Gordon and Betty Moore Foundation's EPIQS Initiative through grant GBMF4534 and by the Department of Energy under grant de-sc0012375. GAF was supported by NSF Grant No. DMR-1949701, NSF Materials Research Science and Engineering Center Grant No. DMR-1720595, and a QuantEmX grant GBMF5305 from ICAM and the Gordon and Betty Moore Foundation.

- <sup>1</sup>J. Mannhart, D. Blank, H. Hwang, A. Millis, and J.-M. Triscone, "Two-dimensional electron gases at oxide interfaces," *Mat. Res. Bull.* **33**, 1027 (2008).
- <sup>2</sup>P. Zubko, S. Gariglio, M. Gabay, P. Ghosez, and J.-M. Triscone, "Interface physics in complex oxide heterostructures," *Ann. Rev. Cond. Mat. Phys.* **2**, 141 (2011).
- <sup>3</sup>C. H. Ahn, A. Bhattacharya, M. D. Ventra, J. N. Eckstein, C. D. Frisbie, M. E. Gershenson, A. M. Goldman, I. H. Inoue, J. Mannhart, A. J. Millis, A. F. Morpurgo, D. Natelson, and J.-M. Triscone, "Electrostatic modification of novel materials," *Rev. Mod. Phys.* **78**, 1185 (2006).
- <sup>4</sup>J. Chakhalian, J. M. Rondinelli, J. Liu, B. A. Gray, M. Kareev, E. J. Moon, N. Prasai, J. L. Cohn, M. Varela, I. C. Tung, M. J. Bedzyk, S. G. Altendorf, F. Strigari, B. Dabrowski, L. H. Tjeng, P. J. Ryan, and J. W. Freeland, "Asymmetric orbital-lattice interactions in ultrathin correlated oxide films," *Phys. Rev. Lett.* **107**, 116805 (2011).
- <sup>5</sup>Z. Huang, Ariando, X. Renshaw Wang, A. Rusydi, J. Chen, H. Yang, and T. Venkatesan, "Interface engineering and emergent phenomena in oxide heterostructures," *Advanced Materials* **30**, 1802439 (2018), <https://onlinelibrary.wiley.com/doi/pdf/10.1002/adma.201802439>.
- <sup>6</sup>H. Boschker and J. Mannhart, "Quantum-matter heterostructures," *Annual Review of Condensed Matter Physics* **8**, 145–164 (2017), <https://doi.org/10.1146/annurev-conmatphys-031016-025404>.
- <sup>7</sup>A. K. Yadav, C. T. Nelson, S. L. Hsu, Z. Hong, J. D. Clarkson, C. M. Schlepütz, A. R. Damodaran, P. Shafer, E. Arenholz, L. R. Dedon, D. Chen, A. Vishwanath, A. M. Minor, L. Q. Chen, J. F. Scott, L. W. Martin, and R. Ramesh, "Observation of polar vortices in oxide superlattices," *Nature* **530**, 198 EP – (2016).
- <sup>8</sup>J. Chakhalian, J. W. Freeland, A. J. Millis, C. Panagopoulos, and J. M. Rondinelli, "Colloquium: Emergent properties hidden in plane view: Strong electronic correlations at oxide interfaces," *Rev. Mod. Phys.* **86**, 1189–1202 (2014).
- <sup>9</sup>R. Pentcheva and W. E. Pickett, "Correlation-driven charge order at the interface between a mott and a band insulator," *Phys. Rev. Lett.* **99**, 016802 (2007).
- <sup>10</sup>R. Pentcheva and W. E. Pickett, "Electronic phenomena at complex oxide interfaces: insights from first principles," *J. Phys.: Cond. Mat.* **22**, 043001 (2010).
- <sup>11</sup>K. M. Rabe, "First-principles calculations of complex metal-oxide materials," *Ann. Rev. Cond. Mat. Phys.* **1**, 211–325 (2010).
- <sup>12</sup>H. L. Stormer, D. C. Tsui, and A. C. Gossard, "The fractional quantum hall effect," *Rev. Mod. Phys.* **71**, S298–S305 (1999).
- <sup>13</sup>A. J. Millis and D. G. Schlom, "Electron-hole liquids in transition-metal oxide heterostructures," *Phys. Rev. B* **82**, 073101 (2010).

- <sup>14</sup>A. Ohtomo and H. Y. Hwang, "A high-mobility electron gas at the  $\text{LaAlO}_3/\text{SrTiO}_3$  heterointerface," *Nature* **427**, 423 (2004).
- <sup>15</sup>S. Okamoto and A. J. Millis, "Electronic reconstruction at an interface between a mott insulator and a band insulator," *Nature* **428**, 630 (2004).
- <sup>16</sup>S. Thiel, G. Hammerl, A. Schmehl, C. W. Schneider, and J. Mannhart, "Tunable quasi-two-dimensional electron gases in oxide heterostructures," *Science* **313**, 1942 (2006).
- <sup>17</sup>J. Chakhalian, J. W. Freeland, H.-U. Habermeier, G. Cristiani, G. Khaliullin, M. van Veenendaal, and B. Keimer, "Orbital reconstruction and covalent bonding at an oxide interface," *Science* **318**, 1115 (2007).
- <sup>18</sup>J. Chakhalian, A. J. Millis, and J. Rondinelli, "Whither the oxide interfaces," *Nat. Mat.* **11**, 92 (2012).
- <sup>19</sup>H. Y. Hwang, Y. Iwasa, M. Kawasaki, B. Keimer, N. Nagaosa, and Y. Tokura, "Emergent phenomena at oxide interfaces," *Nat. Mat.* **11**, 103 (2012).
- <sup>20</sup>A. Tsukazaki, A. Ohtomo, T. Kita, Y. Ohno, H. Ohno, and M. Kawasaki, "Quantum hall effect in polar oxide heterostructures," *Science* **315**, 1388 (2007).
- <sup>21</sup>A. Tsukazaki, S. Akasaka, K. Nakahara, Y. Ohno, H. Ohno, D. Maryenko, A. Ohtomo, and M. Kawasaki, "Observation of the fractional quantum hall effect in an oxide," *Nature Materials* **9**, 889–893 (2010).
- <sup>22</sup>"Superconducting interfaces between insulating oxides," *Science* **317**, 1196 (2007).
- <sup>23</sup>L. Li, C. Richter, J. Mannhart, and R. C. Ashoori, "Coexistence of magnetic order and two-dimensional superconductivity at  $\text{LaAlO}_3/\text{SrTiO}_3$  interfaces," *Nucl. Phys.* **7**, 762 (2011).
- <sup>24</sup>J. A. Bert, B. Kalisky, C. Bell, M. Kim, Y. Hikita, H. Y. Hwang, and K. A. Moler, "Direct imaging of the coexistence of ferromagnetism and superconductivity at the  $\text{LaAlO}_3/\text{SrTiO}_3$  interface," *Nucl. Phys.* **7**, 767 (2011).
- <sup>25</sup>A. Brinkman, M. Huijben, M. van Zalk, J. Huijben, U. Zeitler, J. C. Maan, W. G. van der Wiel, G. Rijnders, D. H. A. Blank, and H. Hilgenkamp, "Magnetic effects at the interface between non-magnetic oxides," *Nat. Mat.* **6**, 493 (2007).
- <sup>26</sup>A. Ramirez, "Oxide electronics emerge," *Science* **315**, 1377 (2007).
- <sup>27</sup>J. Mannhart and D. Schlom, "Oxide interfaces: An opportunity for electronics," *Science* **327**, 1607 (2010).
- <sup>28</sup>D. Xiao, W. Zhu, Y. Ran, N. Nagaosa, and S. Okamoto, "Interface engineering of quantum hall effects in digital heterostructures of transition-metal oxides," *Nat. Comm.* **2**, 596 (2011).
- <sup>29</sup>A. Rüegg, C. Mitra, A. A. Demkov, and G. A. Fiete, "Electronic structure of  $(\text{LaNiO}_3)_2/(\text{LaAlO}_3)_N$  heterostructures grown along [111]," *Phys. Rev. B* **85**, 245131 (2012).
- <sup>30</sup>A. Rüegg, C. Mitra, A. A. Demkov, and G. A. Fiete, "Lattice distortion effects on topological phases in  $(\text{LaNiO}_3)_2/(\text{LaAlO}_3)_N$  heterostructures grown along the [111] direction," *Phys. Rev. B* **88**, 115146 (2013).
- <sup>31</sup>A. Rüegg and G. A. Fiete, "Topological insulators from complex orbital order in transition-metal oxides heterostructures," *Phys. Rev. B* **84**, 201103 (2011).
- <sup>32</sup>F. Wang and Y. Ran, "Nearly flat band with chern number  $c = 2$  on the dice lattice," *Phys. Rev. B* **84**, 241103 (2011).
- <sup>33</sup>J. L. Blok, X. Wan, G. Koster, D. H. A. Blank, and G. Rijnders, "Epitaxial oxide growth on polar (111) surfaces," *Appl. Phys. Lett.* **99**, 151917 (2011).
- <sup>34</sup>G. Herranz, F. Sanchez, N. Dix, M. Scigaj, and J. Fontcuberta, "High mobility conduction at (110) and (111)  $\text{LaAlO}_3/\text{SrTiO}_3$  interfaces," *Sci. Rep.* **2**, 758 (2012).
- <sup>35</sup>S. Middey, D. Meyers, M. Kareev, E. J. Moon, B. A. Gray, X. Liu, J. W. Freeland, and J. Chakhalian, "Epitaxial growth of (111)-oriented  $\text{LaAlO}_3/\text{LaNiO}_3$  ultra-thin superlattices," *Appl. Phys. Lett.* **101**, 261602 (2012).
- <sup>36</sup>G. A. Fiete and A. Rüegg, "Topological phases in oxide heterostructures with light and heavy transition metal ions (invited)," *Journal of Applied Physics* **117**, 172602 (2015), <https://doi.org/10.1063/1.4913933>.
- <sup>37</sup>C. L. Kane and E. J. Mele, "[Z<sub>sub 2</sub>] topological order and the quantum spin hall effect," *Phys. Rev. Lett.* **95**, 146802 (2005).
- <sup>38</sup>C. L. Kane and E. J. Mele, "Quantum spin hall effect in graphene," *Phys. Rev. Lett.* **95**, 226801 (2005).
- <sup>39</sup>F. D. M. Haldane, "Model for a quantum hall effect without landau levels: Condensed-matter realization of the "parity anomaly"," *Phys. Rev. Lett.* **61**, 2015–2018 (1988).
- <sup>40</sup>J. Maciejko and G. A. Fiete, "Fractionalized topological insulators," *Nat. Phys.* **11**, 385 (2015).
- <sup>41</sup>L. Balents, "Spin liquids in frustrated magnets," *Nature* **464**, 199 (2010).
- <sup>42</sup>K.-Y. Yang, W. Zhu, D. Xiao, S. Okamoto, Z. Wang, and Y. Ran, "Possible interaction-driven topological phases in (111) bilayers of  $\text{LaNiO}_3$ ," *Phys. Rev. B* **84**, 201104 (2011).
- <sup>43</sup>D. Doennig, W. E. Pickett, and R. Pentcheva, "Confinement-driven transitions between topological and mott phases in  $(\text{LaNiO}_3)_N/(\text{LaAlO}_3)_M$  (111) superlattices," *Phys. Rev. B* **89**, 121110 (2014).
- <sup>44</sup>Y. Wang, Z. Wang, Z. Fang, and X. Dai, "Interaction-induced quantum anomalous hall phase in (111) bilayer of  $\text{LaCoO}_3$ ," *Phys. Rev. B* **91**, 125139 (2015).
- <sup>45</sup>K. Sun, H. Yao, E. Fradkin, and S. A. Kivelson, "Topological insulators and nematic phases from spontaneous symmetry breaking in 2d fermi systems with a quadratic band crossing," *Phys. Rev. Lett.* **103**, 046811 (2009).
- <sup>46</sup>G. L. Stamokostas and G. A. Fiete, "Mixing of  $t_{2g} - e_g$  orbitals in 4d and 5d transition metal oxides," *Phys. Rev. B* **97**, 085150 (2018).
- <sup>47</sup>A. Arab, X. Liu, O. Köksal, W. Yang, R. U. Chandrasena, S. Middey, M. Kareev, S. Kumar, M.-A. Husanu, Z. Yang, L. Gu, V. N. Strocov, T.-L. Lee, J. Minár, R. Pentcheva, J. Chakhalian, and A. X. Gray, "Electronic structure of a graphene-like artificial crystal of  $\text{NdNiO}_3$ ," *Nano Letters* **19**, 8311–8317 (2019), pMID: 31644875, <https://doi.org/10.1021/acs.nanolett.9b03962>.
- <sup>48</sup>S. Okamoto and D. Xiao, "Transition-metal oxide (111) bilayers," *Journal of the Physical Society of Japan* **87**, 041006 (2018), <https://doi.org/10.7566/JPSJ.87.041006>.
- <sup>49</sup>X. Liu, S. Middey, Y. Cao, M. Kareev, and J. Chakhalian, "Geometrical lattice engineering of complex oxide heterostructures: a designer approach to emergent quantum states," *Materials Research Communications* **6**, 133 (2016).
- <sup>50</sup>J. L. Blok, X. Wan, G. Koster, D. H. A. Blank, and G. Rijnders, "Epitaxial oxide growth on polar (111) surfaces," *Applied Physics Letters* **99**, 151917 (2011), <https://doi.org/10.1063/1.3652701>.
- <sup>51</sup>M. Hu, Q. Zhang, L. Gu, Q. Guo, Y. Cao, M. Kareev, J. Chakhalian, and J. Guo, "Reconstruction-stabilized epitaxy of  $\text{LaCoO}_3/\text{SrTiO}_3$ (111) heterostructures by pulsed laser deposition," *Applied Physics Letters* **112**, 031603 (2018), <https://doi.org/10.1063/1.5006298>.
- <sup>52</sup>S. Middey, P. Rivero, D. Meyers, M. Kareev, X. Liu, Y. Cao, J. W. Freeland, S. Barraza-Lopez, and J. Chakhalian, "Polarity compensation in ultra-thin films of complex oxides: The case of a perovskite nickelate," *Scientific Reports* **4**, 6819 EP – (2014).
- <sup>53</sup>S. Middey, D. Meyers, D. Doennig, M. Kareev, X. Liu, Y. Cao, Z. Yang, J. Shi, L. Gu, P. J. Ryan, R. Pentcheva, J. W. Freeland, and J. Chakhalian, "Mott electrons in an artificial graphenelike crystal of rare-earth nickelate," *Phys. Rev. Lett.* **116**, 056801 (2016).
- <sup>54</sup>A. X. Gray, J. Minár, L. Plucinski, M. Huijben, A. Bostwick, E. Rotenberg, S.-H. Yang, J. Braun, A. Winkelmann, G. Conti, D. Eiteneer, A. Ratatanachata, A. A. Greer, J. Ciston, C. Ophus, G. Rijnders, D. H. A. Blank, D. Doennig, R. Pentcheva, J. B. Kortright, C. M. Schneider, H. Ebert, and C. S. Fadley, "Momentum-resolved electronic structure at a buried interface from soft x-ray standing-wave angle-resolved photoemission," *EPL (Europhysics Letters)* **104**, 17004 (2013).
- <sup>55</sup>V. N. Strocov, M. Kobayashi, X. Wang, L. L. Lev, J. Krempasky, V. V. Rogalev, T. Schmitt, C. Cancellieri, and M. L. Reinle-Schmitt, "Soft-x-ray arpes at the swiss light source: From 3d materials to buried interfaces and impurities," *Synchrotron Radiation News* **27**, 31–40 (2014), <https://doi.org/10.1080/08940886.2014.889550>.
- <sup>56</sup>C. S. Fadley, "X-ray photoelectron spectroscopy and diffraction in the hard x-ray regime: Fundamental considerations and future possibilities," *Nuclear Instruments and Methods in Physics Research Section A: Accelerators, Spectrometers, Detectors and Associated Equipment* **547**, 24 – 41 (2005), proceedings of the Workshop on Hard X-ray Photoelectron Spectroscopy.
- <sup>57</sup>A. X. Gray, C. Papp, S. Ueda, B. Balke, Y. Yamashita, L. Plucinski, J. Minár, J. Braun, E. R. Ylvisaker, C. M. Schneider, W. E. Pickett, H. Ebert, K. Kobayashi, and C. S. Fadley, "Probing bulk electronic structure with hard x-ray angle-resolved photoemission," *Nature Materials* **10**, 759–764 (2011).
- <sup>58</sup>A. Jablonski and C. J. Powell, "Practical expressions for the mean escape depth, the information depth, and the effective attenuation length in auger-electron spectroscopy and x-ray photoelectron spectroscopy," *Journal of Vacuum Science & Technology A* **27**, 253–261 (2009), <https://doi.org/10.1116/1.3071947>.
- <sup>59</sup>G. Kotliar, S. Y. Savrasov, K. Haule, V. S. Oudovenko, O. Parcollet, and

- C. A. Marianetti, "Electronic structure calculations with dynamical mean-field theory," *Rev. Mod. Phys.* **78**, 865–951 (2006).
- <sup>60</sup>A. Stern, "Fractional topological insulators: A pedagogical review," *Annual Review of Condensed Matter Physics* **7**, 349–368 (2016).
- <sup>61</sup>L. Hozoi, H. Gretarsson, J. P. Clancy, B.-G. Jeon, B. Lee, K. H. Kim, V. Yushankhai, P. Fulde, D. Casa, T. Gog, J. Kim, A. H. Said, M. H. Upton, Y.-J. Kim, and J. van den Brink, "Longer-range lattice anisotropy strongly competing with spin-orbit interactions in pyrochlore iridates," *Phys. Rev. B* **89**, 115111 (2014).
- <sup>62</sup>J. S. Gardner, M. J. P. Gingras, and J. E. Greedan, "Magnetic pyrochlore oxides," *Rev. Mod. Phys.* **82**, 53–107 (2010).
- <sup>63</sup>R. Wang, A. Go, and A. J. Millis, "Electron interactions, spin-orbit coupling, and intersite correlations in pyrochlore iridates," *Phys. Rev. B* **95**, 045133 (2017).
- <sup>64</sup>J. W. Harter, Z. Y. Zhao, J.-Q. Yan, D. G. Mandrus, and D. Hsieh, "A parity-breaking electronic nematic phase transition in the spin-orbit coupled metal  $\text{Cd}_2\text{Re}_2\text{O}_7$ ," *Science* **356**, 295–299 (2017), <http://science.sciencemag.org/content/356/6335/295.full.pdf>.
- <sup>65</sup>K.-Y. Yang, Y.-M. Lu, and Y. Ran, "Quantum hall effects in a weyl semimetal: Possible application in pyrochlore iridates," *Phys. Rev. B* **84**, 075129 (2011).
- <sup>66</sup>B.-J. Yang and Y. B. Kim, "Topological insulators and metal-insulator transition in the pyrochlore iridates," *Phys. Rev. B* **82**, 085111 (2010).
- <sup>67</sup>H. Zhang, K. Haule, and D. Vanderbilt, "Metal-insulator transition and topological properties of pyrochlore iridates," *Phys. Rev. Lett.* **118**, 026404 (2017).
- <sup>68</sup>H.-M. Guo and M. Franz, "Three-dimensional topological insulators on the pyrochlore lattice," *Phys. Rev. Lett.* **103**, 206805 (2009).
- <sup>69</sup>M. Kargarian, J. Wen, and G. A. Fiete, "Competing exotic topological insulator phases in transition-metal oxides on the pyrochlore lattice with distortion," *Phys. Rev. B* **83**, 165112 (2011).
- <sup>70</sup>R. Schaffer, E. K.-H. Lee, B.-J. Yang, and Y. B. Kim, "Recent progress on correlated electron systems with strong spin-orbit coupling," *Reports on Progress in Physics* **79**, 094504 (2016).
- <sup>71</sup>F.-Y. Li, Y.-D. Li, Y. B. Kim, L. Balents, Y. Yu, and G. Chen, "Weyl magnons in breathing pyrochlore antiferromagnets," *Nature Communications* **7**, 12691 EP – (2016).
- <sup>72</sup>W. Witczak-Krempa and Y. B. Kim, "Topological and magnetic phases of interacting electrons in the pyrochlore iridates," *Phys. Rev. B* **85**, 045124 (2012).
- <sup>73</sup>X. Wan, A. M. Turner, A. Vishwanath, and S. Y. Savrasov, "Topological semimetal and fermi-arc surface states in the electronic structure of pyrochlore iridates," *Phys. Rev. B* **83**, 205101 (2011).
- <sup>74</sup>J. Maciejko, V. Chua, and G. A. Fiete, "Topological order in a correlated three-dimensional topological insulator," *Phys. Rev. Lett.* **112**, 016404 (2014).
- <sup>75</sup>D. Pesin and L. Balents, "Mott physics and band topology in materials with strong spin-orbit coupling," *Nat. Phys.* **6**, 376 (2010).
- <sup>76</sup>N. P. Armitage, E. J. Mele, and A. Vishwanath, "Weyl and dirac semimetals in three-dimensional solids," *Rev. Mod. Phys.* **90**, 015001 (2018).
- <sup>77</sup>X.-G. Wen, *Quantum Field Theory of Many-Body Systems* (Oxford, New York, 2004).
- <sup>78</sup>M. Z. Hasan and C. L. Kane, "Colloquium: Topological insulators," *Rev. Mod. Phys.* **82**, 3045–3067 (2010).
- <sup>79</sup>J. E. Moore, "The birth of topological insulators," *Nature* **464**, 194 (2010).
- <sup>80</sup>X.-L. Qi and S.-C. Zhang, "Topological insulators and superconductors," *Rev. Mod. Phys.* **83**, 1057–1110 (2011).
- <sup>81</sup>L. Fu, "Topological crystalline insulators," *Phys. Rev. Lett.* **106**, 106802 (2011).
- <sup>82</sup>T. H. Hsieh, H. Lin, J. Liu, W. Duan, A. Bansil, and L. Fu, "Topological crystalline insulators in the snite material class," *Nat. Commun.* **3**, 982 (2012).
- <sup>83</sup>X. Liu, M. Karem, Y. Cao, J. Liu, S. Middey, D. Meyers, J. W. Freeland, and J. Chakhalian, "Electronic and magnetic properties of (1 1 1)-oriented  $\text{CoCr}_2\text{O}_4$  epitaxial thin film," (2014), [arXiv:1406.0523](https://arxiv.org/abs/1406.0523).
- <sup>84</sup>K. Shiozaki, M. Sato, and K. Gomi, "Topology of nonsymmorphic crystalline insulators and superconductors," *Phys. Rev. B* **93**, 195413 (2016).
- <sup>85</sup>A. P. Schnyder, S. Ryu, A. Furusaki, and A. W. W. Ludwig, "Classification of topological insulators and superconductors in three spatial dimensions," *Phys. Rev. B* **78**, 195125 (2008).
- <sup>86</sup>S. Ryu, A. P. Schnyder, A. Furusaki, and A. W. W. Ludwig, "Topological insulators and superconductors: ten-fold way and dimensional hierarchy," *New J. Phys.* **12**, 065010 (2010).
- <sup>87</sup>S. M. Young, S. Zaheer, J. C. Y. Teo, C. L. Kane, E. J. Mele, and A. M. Rappe, "Dirac semimetal in three dimensions," *Phys. Rev. Lett.* **108**, 140405 (2012).
- <sup>88</sup>J. A. Steinberg, S. M. Young, S. Zaheer, C. L. Kane, E. J. Mele, and A. M. Rappe, "Bulk dirac points in distorted spinels," *Phys. Rev. Lett.* **112**, 036403 (2014).
- <sup>89</sup>L. Fu, C. L. Kane, and E. J. Mele, "Topological insulators in three dimensions," *Phys. Rev. Lett.* **98**, 106803 (2007).
- <sup>90</sup>S. Murakami, S. Iso, Y. Avishai, M. Onoda, and N. Nagaosa, "Tuning phase transition between quantum spin hall and ordinary insulating phases," *Phys. Rev. B* **76**, 205304 (2007).
- <sup>91</sup>B.-J. Yang and N. Nagaosa, "Emergent topological phenomena in thin films of pyrochlore iridates," *Phys. Rev. Lett.* **112**, 246402 (2014).
- <sup>92</sup>X. Hu, A. Ruegg, and G. A. Fiete, "Topological phases in layered pyrochlore oxide thin films along the [111] direction," *Phys. Rev. B* **86**, 235141 (2012).
- <sup>93</sup>X. Hu, Z. Zhong, and G. A. Fiete, "First principles prediction of topological phases in thin films of pyrochlore iridates," *Sci. Rep.* **5**, 11072 (2015).
- <sup>94</sup>K. Hwang and Y. B. Kim, "Theory of multifarious quantum phases and large anomalous hall effect in pyrochlore iridate thin films," *Scientific Reports* **6**, 30017 EP – (2016).
- <sup>95</sup>Q. Chen, H.-H. Hung, X. Hu, and G. A. Fiete, "Correlation effects in pyrochlore iridate thin films grown along the [111] direction," *Phys. Rev. B* **92**, 085145 (2015).
- <sup>96</sup>P. Laurell and G. A. Fiete, "Topological magnon bands and unconventional superconductivity in pyrochlore iridate thin films," *Phys. Rev. Lett.* **118**, 177201 (2017).
- <sup>97</sup>O. Köksal, S. Baidya, and R. Pentcheva, "Confinement-driven electronic and topological phases in corundum-derived 3d-oxide honeycomb lattices," *Phys. Rev. B* **97**, 035126 (2018).
- <sup>98</sup>S. Okamoto, W. Zhu, Y. Nomura, R. Arita, D. Xiao, and N. Nagaosa, "Correlation effects in (111) bilayers of perovskite transition-metal oxides," *Phys. Rev. B* **89**, 195121 (2014).
- <sup>99</sup>Q.-F. Liang, L.-H. Wu, and X. Hu, "Electrically tunable topological state in [111] perovskite materials with an antiferromagnetic exchange field," *New Journal of Physics* **15**, 063031 (2013).
- <sup>100</sup>J. L. Lado, V. Pardo, and D. Baldomir, "Ab initio study of z2 topological phases in perovskite (111) ( $\text{SrTiO}_3$ )/( $\text{SrIrO}_3$ )<sub>2</sub> and ( $\text{KTaO}_3$ )/( $\text{KPtO}_3$ )<sub>2</sub> multilayers," *Phys. Rev. B* **88**, 155119 (2013).
- <sup>101</sup>R. Oja, K. Johnston, J. Frantti, and R. M. Nieminen, "Computational study of (111) epitaxially strained ferroelectric perovskites  $\text{BaTiO}_3$  and  $\text{PbTiO}_3$ ," *Phys. Rev. B* **78**, 094102 (2008).
- <sup>102</sup>S. Okamoto, "Doped mott insulators in (111) bilayers of perovskite transition-metal oxides with a strong spin-orbit coupling," *Phys. Rev. Lett.* **110**, 066403 (2013).
- <sup>103</sup>B. Ye, A. Mesaros, and Y. Ran, "Possible correlation-driven odd-parity superconductivity in  $\text{LaNi}_{7/8}\text{Co}_{1/8}\text{O}_3$  (111) bilayers," *Phys. Rev. B* **89**, 201111 (2014).
- <sup>104</sup>M. Moreau, A. Marthinsen, S. M. Selbach, and T. Tybell, "Strain-phonon coupling in (111)-oriented perovskite oxides," *Phys. Rev. B* **96**, 094109 (2017).
- <sup>105</sup>F. Cossu, H. A. Tahini, N. Singh, and U. Schwingenschlögl, "Charge driven metal-insulator transitions in  $\text{LaMnO}_3/\text{SrTiO}_3$ (111) superlattices," *EPL (Europhysics Letters)* **118**, 57001 (2017).
- <sup>106</sup>H. A. Tahini, F. Cossu, N. Singh, S. C. Smith, and U. Schwingenschlögl, "Electronic phase transitions under hydrostatic pressure in  $\text{LaNO}_3$  (111) bilayers sandwiched between  $\text{LaAlO}_3$ ," *Phys. Rev. B* **93**, 035117 (2016).
- <sup>107</sup>J. J. Ishikawa, E. C. T. O'Farrell, and S. Nakatsuji, "Continuous transition between antiferromagnetic insulator and paramagnetic metal in the pyrochlore iridate  $\text{Eu}_2\text{Ir}_2\text{O}_7$ ," *Phys. Rev. B* **85**, 245109 (2012).
- <sup>108</sup>S.-W. Kim, S.-H. Kwon, D.-K. Kwak, and S.-W. Kang, "Phase control of iridium and iridium oxide thin films in atomic layer deposition," *Journal of Applied Physics* **103**, 023517 (2008).
- <sup>109</sup>H. Jehn, R. Volker, and M. Ismail, "Iridium losses during oxidation," *Platinum Metals Rev.* **22**, 92 (1978).
- <sup>110</sup>J. C. Chaston, "Reactions of oxygen with the platinum metals," *Platinum*



- Metals Rev. **9**, 51 (1965).
- <sup>112</sup>J. C. Gallagher, B. D. Esser, R. Morrow, S. R. Dunsiger, R. E. A. Williams, P. M. Woodward, D. W. McComb, and F. Y. Yang, "Epitaxial growth of iridate pyrochlore  $\text{Nd}_2\text{Ir}_2\text{O}_7$  films," *Scientific Reports* **6**, 22282 (2016).
- <sup>113</sup>W. J. Kim, J. H. Gruenewald, T. Oh, S. Cheon, B. Kim, O. B. Korneta, H. Cho, D. Lee, Y. Kim, M. Kim, J.-G. Park, B.-J. Yang, A. Seo, and T. W. Noh, "Unconventional anomalous hall effect from antiferromagnetic domain walls of  $\text{Nd}_2\text{Ir}_2\text{O}_7$  thin films," *Phys. Rev. B* **98**, 125103 (2018).
- <sup>114</sup>T. C. Fujita, Y. Kozuka, M. Uchida, A. Tsukazaki, T. Arima, and M. Kawasaki, "Odd-parity magnetoresistance in pyrochlore iridate thin films with broken time-reversal symmetry," *Scientific Reports* **5**, 9711 (2015).
- <sup>115</sup>T. C. Fujita, M. Uchida, Y. Kozuka, S. Ogawa, A. Tsukazaki, T. Arima, and M. Kawasaki, "All-in-all-out magnetic domain size in pyrochlore iridate thin films as probed by local magnetotransport," *Applied Physics Letters* **108**, 022402 (2016).
- <sup>116</sup>Y. Kozuka, T. C. Fujita, M. Uchida, T. Nojima, A. Tsukazaki, J. Matsuno, T. Arima, and M. Kawasaki, "Visualizing ferroic domains in an all-in-all-out antiferromagnet thin film," *Phys. Rev. B* **96**, 224417 (2017).
- <sup>117</sup>T. C. Fujita, Y. Kozuka, J. Matsuno, M. Uchida, A. Tsukazaki, T. Arima, and M. Kawasaki, "All-in-all-out magnetic domain inversion in  $\text{tb}_2\text{Ir}_2\text{O}_7$  with molecular fields antiparallel to external fields," *Phys. Rev. Materials* **2**, 011402 (2018).
- <sup>118</sup>T. Ohtsuki, Z. Tian, A. Endo, M. Halim, S. Katsumoto, Y. Kohama, K. Kindo, M. Lippmaa, and S. Nakatsuji, "Strain-induced spontaneous hall effect in an epitaxial thin film of a luttinger semimetal," *Proceedings of the National Academy of Sciences* **116**, 8803–8808 (2019), <https://www.pnas.org/content/116/18/8803.full.pdf>.
- <sup>119</sup>L. Guo, N. Campbell, Y. Choi, J.-W. Kim, P. J. Ryan, H. Huyan, L. Li, T. Nan, J.-H. Kang, C. Sundahl, X. Pan, M. S. Rzchowski, and C.-B. Eom, "Spontaneous hall effect enhanced by local ir moments in epitaxial  $\text{pr}_2\text{Ir}_2\text{O}_7$  thin films," (2019), arXiv:1912.12401 [cond-mat.mtrl-sci].
- <sup>120</sup>T. Ohtsuki, Z. Tian, M. Halim, S. Nakatsuji, and M. Lippmaa, "Growth of  $\text{pr}_2\text{Ir}_2\text{O}_7$  thin films using solid phase epitaxy," *Journal of Applied Physics* **127**, 035303 (2020).
- <sup>121</sup>W. C. Yang, Y. T. Xie, W. K. Zhu, K. Park, A. P. Chen, Y. Losovyj, Z. Li, H. M. Liu, M. Starr, J. A. Acosta, C. G. Tao, N. Li, Q. X. Jia, J. J. Heremans, and S. X. Zhang, "Epitaxial thin films of pyrochlore iridate  $\text{bi}_2\text{xir}_2\text{-yo}_7$ ?: structure, defects and transport properties," *Scientific Reports* **7**, 7740 (2017).
- <sup>122</sup>W. C. Yang, Y. T. Xie, X. Sun, X. H. Zhang, K. Park, S. C. Xue, Y. L. Li, C. G. Tao, Q. X. Jia, Y. Losovyj, H. Wang, J. J. Heremans, and S. X. Zhang, "Stoichiometry control and electronic and transport properties of pyrochlore  $\text{Bi}_2\text{Ir}_2\text{O}_7$  thin films," *Phys. Rev. Materials* **2**, 114206 (2018).
- <sup>123</sup>J.-H. Chu, J. Liu, H. Zhang, K. Noordhoek, S. C. Riggs, M. Shapiro, C. R. Serro, D. Yi, M. Mellisa, S. J. Suresha, C. Frontera, E. Arenholz, A. Vishwanath, X. Marti, I. R. Fisher, and R. Ramesh, "Possible scale invariant linear magnetoresistance in pyrochlore iridates  $\text{bi}_2\text{Ir}_2\text{O}_7$ ," *New Journal of Physics* **21**, 113041 (2019).
- <sup>124</sup>T. C. Fujita, M. Uchida, Y. Kozuka, W. Sano, A. Tsukazaki, T. Arima, and M. Kawasaki, "All-in-all-out magnetic domain wall conduction in a pyrochlore iridate heterointerface," *Phys. Rev. B* **93**, 064419 (2016).
- <sup>125</sup>W. Witczak-Krempa, G. Chen, Y. B. Kim, and L. Balents, "Correlated quantum phenomena in the strong spin-orbit regime," *Annual Review of Condensed Matter Physics* **5**, 57–82 (2014).
- <sup>126</sup>T.-h. Arima, "Time-reversal symmetry breaking and consequent physical responses induced by all-in-all-out type magnetic order on the pyrochlore lattice," *Journal of the Physical Society of Japan* **82**, 013705 (2013).
- <sup>127</sup>K. Ueda, J. Fujioka, B.-J. Yang, J. Shiozaki, A. Tsukazaki, S. Nakamura, S. Awaji, N. Nagaosa, and Y. Tokura, "Magnetic field-induced insulator-semimetal transition in a pyrochlore  $\text{Nd}_2\text{Ir}_2\text{O}_7$ ," *Phys. Rev. Lett.* **115**, 056402 (2015).
- <sup>128</sup>Y. Machida, S. Nakatsuji, S. Onoda, T. Tayama, and T. Sakakibara, "Time-reversal symmetry breaking and spontaneous hall effect without magnetic dipole order," *Nature* **463**, 210–213 (2010).
- <sup>129</sup>S. K. Choi, R. Coldea, A. N. Kolmogorov, T. Lancaster, I. I. Mazin, S. J. Blundell, P. G. Radaelli, Y. Singh, P. Gegenwart, K. R. Choi, S.-W. Cheong, P. J. Baker, C. Stock, and J. Taylor, "Spin waves and revised crystal structure of honeycomb iridate  $\text{Na}_2\text{Ir}_2\text{O}_7$ ," *Phys. Rev. Lett.* **108**, 127204 (2012).
- <sup>130</sup>L. J. P. Ament, M. van Veenendaal, T. P. Devereaux, J. P. Hill, and J. van den Brink, "Resonant inelastic x-ray scattering studies of elementary excitations," *Rev. Mod. Phys.* **83**, 705–767 (2011).
- <sup>131</sup>M. Dzero, J. Xia, V. Galitski, and P. Coleman, "Topological kondo insulators," *Annual Review of Condensed Matter Physics* **7**, 249–280 (2016), <https://doi.org/10.1146/annurev-conmatphys-031214-014749>.
- <sup>132</sup>X. Liu, S. Singh, B. J. Kirby, Z. Zhong, Y. Cao, B. Pal, M. Kareev, S. Middey, J. W. Freeland, P. Shafer, E. Arenholz, D. Vanderbilt, and J. Chakhalian, "Emergent magnetic state in (111)-oriented quasi-two-dimensional spinel oxides," *Nano Letters* **19**, 8381–8387 (2019), pMID: 31665887, <https://doi.org/10.1021/acs.nanolett.9b02159>.
- <sup>133</sup>"Introduction to frustrated magnetism," *Springer Series in Solid-State Sciences* (2011), 10.1007/978-3-642-10589-0.